frontiers in Materials

ORIGINAL RESEARCH
published: 11 February 2020
doi: 10.3389/fmats.2020.00013

Simultaneously Enhancing Thermal Stable Dielectric Property and Piezoelectric Response in Lead-Free $LiNbO_3$-Modified $(K_{0.5}Na_{0.5})NbO_3$-$(BaNi_{0.5}Nb_{0.5}O_3)$ System

Hongfen Ji[1], Lipeng Xin[2]*, Han Ma[1], Weiguo Liu[1], Zhonghua Dai[1], Lixia Pang[1], Jinglong Xie[1] and Zhaobin Chen[1]*

[1] *Laboratory of Thin Film Techniques and Optical Test, School of Photoelectrical Engineering, Xi'an Technological University, Xi'an, China,* [2] *Frontier Institute of Science and Technology, Xi'an Jiaotong University, Xi'an, China*

OPEN ACCESS

Edited by:
Rajesh Adhikari,
Institut National de la Recherche Scientifique (INRS), Canada

Reviewed by:
Jigong Hao,
Liaocheng University, China
Laijun Liu,
Guilin University of Technology, China

***Correspondence:**
Hongfen Ji
jihongfen@126.com
Lipeng Xin
ybsyh3@163.com

Specialty section:
This article was submitted to Functional Ceramics, a section of the journal Frontiers in Materials

Received: *27 October 2019*
Accepted: *14 January 2020*
Published: *11 February 2020*

Citation:
Ji H, Xin L, Ma H, Liu W, Dai Z, Pang L, Xie J and Chen Z (2020) Simultaneously Enhancing Thermal Stable Dielectric Property and Piezoelectric Response in Lead-Free $LiNbO_3$-Modified $(K_{0.5}Na_{0.5})NbO_3$-$(BaNi_{0.5}Nb_{0.5}O_3)$ System. Front. Mater. 7:13. doi: 10.3389/fmats.2020.00013

Perovskite ferroelectic oxides with simultaneous highly thermal stable dielectric property and piezoelectric response are promising candidate for advanced energy, dielectric, and smart devices. The (1-x)[0.98[$(K_{0.5}Na_{0.5})NbO_3$]-0.02($BaNi_{0.5}Nb_{0.5}O_3$)]-x$LiNbO_3$ (abbreviated as (1-x)KNBNNO-x$LiNbO_3$; x = 0.00, 0.02, 0.04, 0.06, 0.08) lead-free multifunction ferroelectric ceramic is synthesized by solid-state reaction method. XRD analysis reveals that the samples exhibit perovskite structure with $0 \leq x \leq 0.06$, and the second phase $K_3Li_2Nb_5O_{15}$ appears at x = 0.08. The scanning electron microscopy image show that the grain size of ceramics increases from 0.65 to 3.58 μm with $LiNbO_3$ content increasing. Meanwhile, the Curie temperature (T_C) shifts to a higher temperature (∼ 427°C for x = 0.06). A high dielectric thermal stability of $\Delta\varepsilon/\varepsilon_{40^\circ C} \leq \pm 10\%$, with a high dielectric permittivity (∼1,400), is achieved at x = 0.06 over a wide temperature range of ∼40–348°C with d_{33} of ∼160 $pC{\cdot}N^{-1}$, and a remnant polarization (P_r) of 20.5 $\mu C{\cdot}cm^{-2}$. This work shows that this multifunction material could be applied in sensor to efficiently covert both solar and kinetic energies into electricity over a wide temperature range.

Keywords: piezoelectrics, dielectric temperature stability, morphotropic phase boundary (MPB), lead-free, perovskite, ceramics, oxides

INTRODUCTION

Perovskite oxides, with the ABO_3 topological structure, have been recognized as the smart platform for the next generation advanced multifunctional energy conversion and/or storage devices (Bai et al., 2017, 2019; Hao et al., 2019). In particular, the subgroup of ferroelectric perovskite materials, with non-centrosymmetric crystallographic structure (Glazer, 1975), are appealing for these multifunctional devices due to their inherent multi-stimuli responsive characteristics. The ferroelectrics are sensitive to external and/or internal stimuli, such as temperature, light, magnetic field, stress, and chemical doping (Bai et al., 2018; Zheng et al., 2018), owing to their highly structural tolerance. Very recently, various types of ferroelectric systems have been used for these promising applications. For example, $Pb(Zr_{0.53}Ti_{0.47})O_3$ ceramics mediated with $Pb(Fe_{0.5}Ta_{0.5})O_3$ or $PbTiO_3$-$0.35Bi(Ni_{2/3+x}Nb_{1/3-x})O_{3-\delta}$ ceramics (Evans et al., 2013; Liu et al., 2015), (1-x)$KNbO_3$-x$BaNi_{1/2}Nb_{1/2}O_{3-\delta}$ (KBNNO) ceramics (Bai et al., 2019), (1–x)

$Na_{0.5}Bi_{0.5}TiO_3$-xBa($Ti_{0.5}Ni_{0.5}$)$O_{3-\delta}$ ceramics (Xiao et al., 2019), and ($K_{0.5}Na_{0.5}$)NbO_3 doped with 2 mol% Ba($Ni_{0.5}Nb_{0.5}$)$O_{3-\delta}$ ceramics (KNBNNO ceramics) (Bai et al., 2017; Zhong et al., 2019).

However, lead-based ceramics have urgent toxicity for the environment and/or human development due to their intrinsic volatility under extreme conditions (Hong et al., 2016; Zheng et al., 2018). The emerging of ($K_{0.5}Na_{0.5}$)NbO_3 (KNN)-based lead-free system would be a remarkable alternative for these drawbacks due to its high-performance piezoelectric, ferroelectric properties, and high curie temperature (Du et al., 2007b; Ding et al., 2018; Zhao et al., 2019). Furthermore, the piezoelectricity and temperature stability substantially determine the macroscopical performance of ferroelectric materials (Zhao et al., 2007; Sun et al., 2016; Yan et al., 2017, 2018c). According to the structure-activity relationship, chemical modification is an effective method to enhance the temperature stability and piezoelectric properties of KNN-based ceramics, including the formation of solid solutions with other compounds, such as $LiNbO_3$ (Wang and Li, 2010a; Long et al., 2016), $LiTaO_3$ (Chang et al., 2007; Zhao et al., 2007), $LiSbO_3$ (Shi et al., 2014), $BaTiO_3$ (Kim et al., 2016), $Bi_{0.5}Na_{0.5}TiO_3$ (Zuo et al., 2007; Liu et al., 2014, 2017), or a combination of multiple additives (Mazhao et al., 2015). Among them, the lithium niobate ($LiNbO_3$), not composing of the expensive Ta and toxic Sb elements, could simultaneously increase the piezoelectric coefficient (d_{33}) and the Curie temperature (T_C) instead of sacrificing T_C for a higher d_{33}. Moreover, the Li ion is beneficial to reduce the sintering temperature of ceramics (Wang and Li, 2010a). Unfortunately, few studies have focus to the thermal stability of KNN-based functional ceramics, which is the pivotal parameter for practical device working. Therefore, it is of great interest to design KNN-based multifunction materials with both improved piezoelectricity properties and favored temperature stability. The KNBNNO system is a kind of excellent multifunctional ferroelectric material with narrower bandgap (1.6 eV), large piezoelectric coefficient (100 $pC \cdot N^{-1}$), large pyroelectric coefficient (130 $\mu C \cdot K^{-1} \cdot m^{-2}$) but smaller remanent polarization (11.3 $\mu C \cdot cm^{-2}$). The synergetic enhancement of as-mentioned piezoelectricity and thermal stability would make this system to be a paradigm for smart platform applications (Bai et al., 2017).

In this work, (1-x)[0.98[($K_{0.5}Na_{0.5}$)NbO_3]-0.02($BaNi_{0.5}Nb_{0.5}O_3$)]-x$LiNbO_3$ (abbreviated as (1-x)KNBNNO-x$LiNbO_3$; x = 0.00, 0.02, 0.04, 0.06, 0.08) ceramics were prepared by solid-state reaction method through A-site substitution by Li^+. The results show that both piezoelectricity and thermal stability of KNBNNO-$LiNbO_3$ system can be enhanced simultaneously. The underlying physical picture regarding these properties is the appearing of morphotropic phase boundary (MPB) between orthorhombic and tetragonal phases by $LiNbO_3$ doping. Furthermore, the phase structure, surface morphology, and electric properties (such as dielectric, ferroelectric and piezoelectric properties) were studied. This work would promote the development of lead-free multifunctional ferroelectrics over a broad temperature range.

MATERIALS AND METHODS

Materials

KNBNNO-$LiNbO_3$ lead-free ceramics were synthesized by solid-state reaction method using the analysis reagent of oxides and carbonates: Na_2CO_3 (99.8%), K_2CO_3 (99.0%), Nb_2O_5 (99.5%), Li_2CO_3 (98.0%), $BaCO_3$ (99.0%), and NiO (98.0%). The powders were mixed by stoichiometric ratio, then ball-milled in ethanol with stabilized zirconia media for 12 h. After drying at 90°C, the powder was calcined at 850°C for 3 h using alumina crucibles before milled for 12 h. The 6 wt.% PVA was mixed into the powders after drying and sieving, and the pellets were pressed at 200 MPa. Finally, the pressed disks were sintered between 1,040°C and 1,180°C for 2 h. In order to weaken the evaporation of alkalis during sintering, the disks were embedded in precursor powders.

Methods

The bulk densities were obtained by Archimedes' Method. The phase structure of samples was measured using X-ray diffraction spectrometry (XRD, Shimadzu, LabX XRD-600) with Cu-Kα radiation (λ = 1.54056 Å). The morphology and grain size were investigated using scanning electron microscopy (SEM, JEOL, JSM EMP-800 Tokyo). The remaining disks were polished and coated with high temperature sliver electrodes for electrical property analysis. The dielectric property was measured at 10 kHz using an LCR meter (Agilent, Agilent 4980A, Santa Clara) from 40°C to 480°C, while the ferroelectric property was measured using a ferroelectric analyzer (axiACCT, TF-2000, Germany). The piezoelectric coefficient d_{33} was measured by Berlincourt-type quasi-static meter, before that, the samples were poled at 150°C for 30 min in silicon oil, then keep pressure and cool to room temperature for testing, the poling electric field was 40 kV/cm.

RESULTS AND DISCUSSION

The XRD patterns of KNBNNO-$x$$LiNbO_3$ solid solution with $0 \le x \le 0.08$ at room temperature are shown in **Figure 1A**. Only pure perovskite structure is formed at $0 \le x \le 0.06$, and the original diffraction peak moves toward lower angles upon the increasing of x. This characteristic could be attributed to the K^+ (1.33 Å) and Na^+ (0.97 Å) ions are substituted by Li^+ (0.90 Å) ions at the A-site of perovskite structure (Wang and Li, 2007). However, the second phase of tetragonal tungsten bronze $K_3Li_2Nb_5O_{15}$ (ICDD: 52-0157) appears when $x = 0.08$. This phenomenon results from the limited solid solubility of Li into the A-sites of KNBNNO, and the different space group between KNN (*Amm*2) and $LiNbO_3$ (*R*3*c*) (Yan et al., 2004).

The relatively integrated intensity of the enlarged XRD patterns between 44° and 47° were fitted using the Lorentz function (see **Figure 1B**). It deserves to be noted that the theoretical ratio of I(200) / I(002) is 1:2 and 2:1 for an orthorhombic and tetragonal phase, respectively (Liu et al., 2012). Therefore, the pure KNBNNO sample is orthorhombic phase according to the fitting data (Cheng et al., 2012). However, the intensity ratio of I(200) / I(002) gradually raises with the increasing of doping content. It implies that the obtained phase is combined with orthorhombic and tetragonal phases when $x = 0.02–0.06$ (Liu et al., 2012). This is because the integrated intensity of these two peaks approaches to ~ 1 (Zhang et al., 2006). In this regard, a MPB region has been established in the range of $x = 0.02–0.06$, which would significantly affect the piezoelectric and dielectric properties (Saito and Takao, 2006). The discrepancy of (002) peaks at x = 0.06 might be due to the mild texturing that formed on the surface of solid solution, as proved in **Figure 2C**. When $x = 0.08$, the tetragonal phase is appeared with an intensity ratio of $\sim$ 2:1.

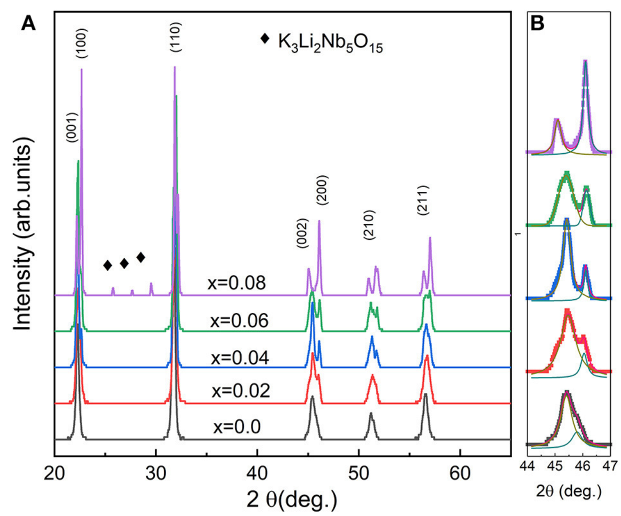

FIGURE 1 | (A) XRD patterns of (1-*x*)KNBNNO-*x*LiNbO$_3$ ceramics (x = 0–0.08); **(B)** enlarged XRD patterns for $2\theta = 44–47°$.

Figure 2 shows the morphology of the (1-*x*)KNNBNNO-*x*LiNbO$_3$ solid solution with various x values sintered at their optimized temperatures. It demonstrates most of the regular rectangular grains surrounded by tiny grains. The average grain size increases from $\sim$ 0.65 µm ($x = 0.00$) to $\sim$ 3.58 µm ($x = 0.08$) with increasing LiNbO$_3$ content. Besides, the high relative density (>96%) has been obtained. Specifically, the densities of as-synthesized ceramics first increase from 4.35 g·cm^{-3} (x = 0.00) to 4.46 g·cm^{-3} (x = 0.06), and then decreased to 4.33 g·cm^{-3} at $x = 0.08$. The substitution of Li ions would promote the formation of a transient liquid phase during the sintering process, which could benefit grain growth and compact structure (Zhao et al., 2019). The reason for the decrease in density may be due to the appearance of a low-density second phase $K_3Li_2Nb_5O_{15}$ (theoretical density: 4.376 g·cm^{-3}).

The effect of temperature on the dielectric properties at 10 kHz for unpoled (1-*x*)KNBNNO-*x*LiNbO$_3$ ceramics with $0 \leq x \leq 0.08$ is shown in **Figure 3a**. Two dielectric peaks are observed from 40°C to 480°C, corresponding to the phase transition temperatures, from the orthorhombic phase to the tetragonal phase (marked as T_{O-T}) and from the tetragonal phase to the cubic phase (marked as T_C), respectively (Zhang et al., 2006; Hao et al., 2015). Meanwhile, the inverse dielectric constant (1/ε) as a function of temperature at 10 kHz has

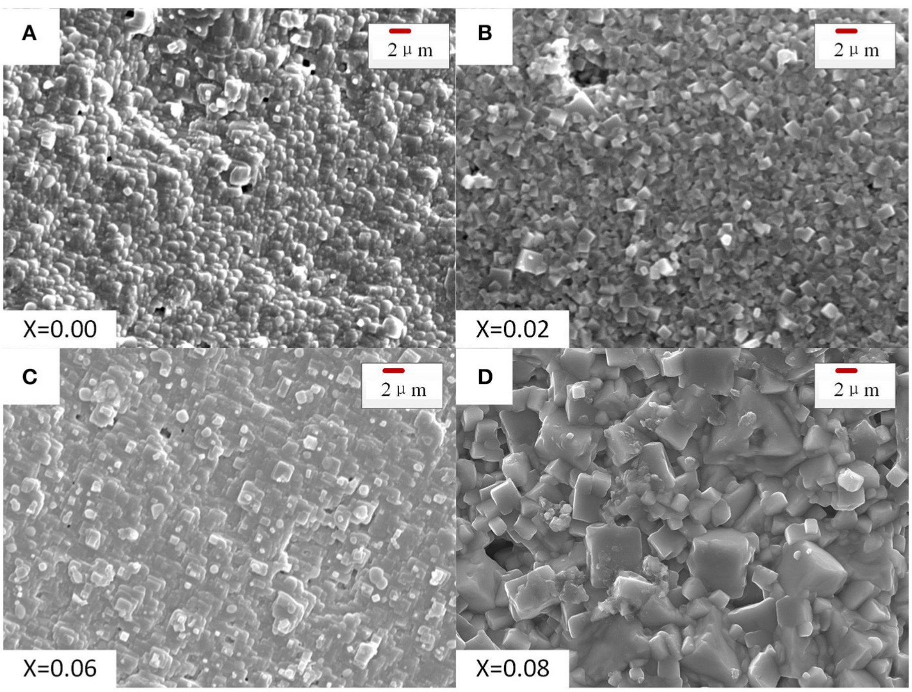

FIGURE 2 | SEM images of (1-*x*)KNBNNO-*x*LiNbO$_3$ ceramics for **(A)** $x = 0.00$, **(B)** $x = 0.02$, **(C)** $x = 0.06$, and **(D)** $x = 0.08$.

been clearly shown in **Figure 3b**. The dielectric permittivity above the curie point follows the Curie-Weiss law, as shown in Equation (1).

$$\varepsilon_r = C/(T - T_0); \quad (T > T_0) \tag{1}$$

where T_0 is the Curie-Weiss temperature and C is the Curie Weiss constant. And the Curie point T_C can be got from the curve (Bokov and Ye, 2012). The T_{O-T} also corresponds with another peak of the curve. The phase transition temperature of pure KNBNNO ($x = 0.00$) ceramics can be observed at $T_C = 375.5°C$ and $T_{O-T} = 148.5°C$, respectively. Interestingly, the ceramics at $x = 0.06$ shows the lowest T_{O-T} value, being near to room temperature, and a highest T_C, close to 427°C. Overall, the T_{O-T} decreases largely from 148.5°C to 57°C, while the T_C increases from 375.5°C to 423°C with the increasing $LiNbO_3$ content ($0 \leq x \leq 0.06$). It is likely due to the smaller radius of the Li ion than that of the K and Na ions, consequentially, the tolerance factor of the perovskite structure decreases upon increasing *x*. Therefore, the tetragonal distortion of the sample should be enhanced, where T_C shifts to a higher temperature, while T_{O-T} moves to a lower temperature, as shown in **Figure 3c** (Yan et al., 2018a,b). Furthermore, both the high T_C of $LiNbO_3$ (∼1,200°C) and the large crystal anisotropy could also induce this effect (Acosta et al., 2017).

Figure 3d illustrates the thermal stability of the relative permittivity ($\Delta\varepsilon/\varepsilon_{\ 40°C}$) between 40°C and 400°C for the (1-*x*)KNBNNO-*x*$LiNbO_3$ (x = 0.00–0.08) ceramics at

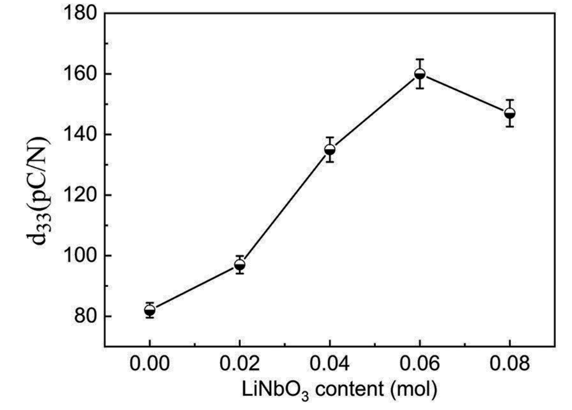

FIGURE 4 | Piezoelectric properties for (1-*x*)KNBNNO-*x*$LiNbO_3$ (x = 0.00–0.08) ceramics.

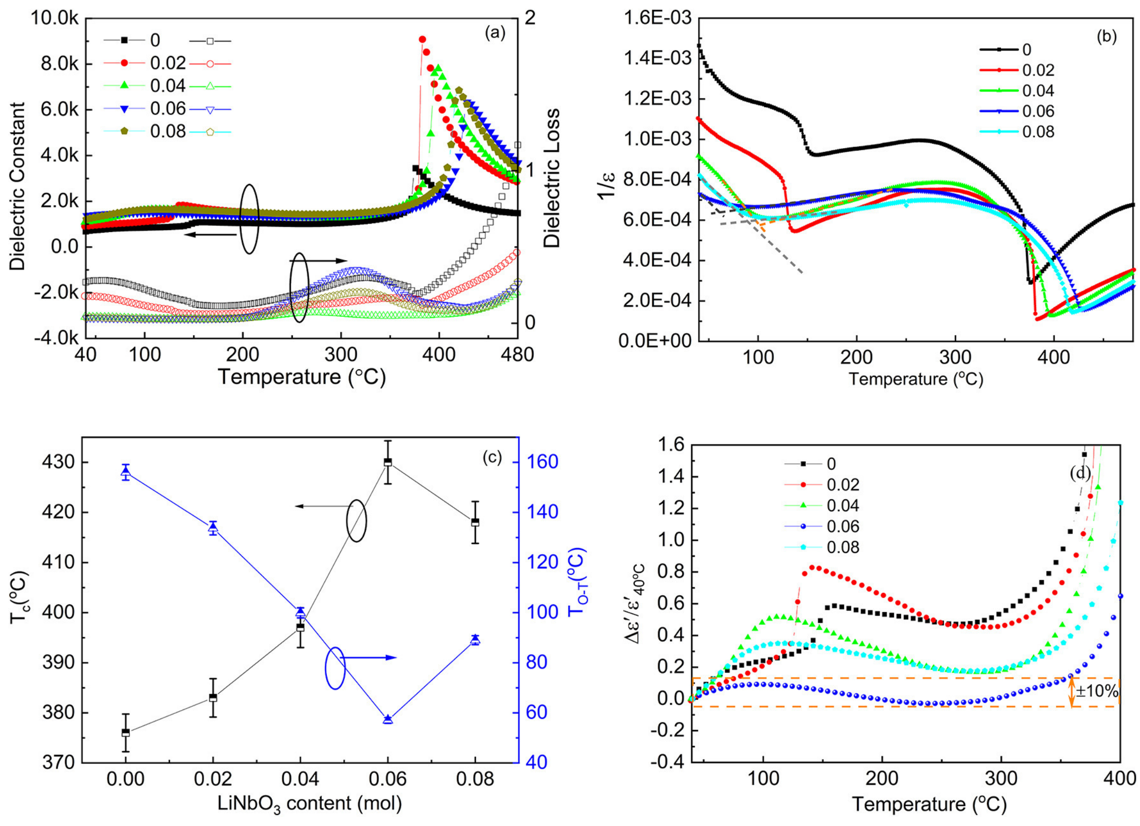

FIGURE 3 | (a) Effect of temperature on the dielectric properties at 10 kHz for KNBNNO-x$LiNbO_3$ ceramics with $0 \leq x \leq 0.08$; **(b)** the inverse dielectric constant (1/ε) varies with temperature at 10 kHz; **(c)**T_C and T_{O-T} change with $LiNbO_3$ content; **(d)** Thermal stability of the relative permittivity ($\Delta\varepsilon/\varepsilon_{40°C}$) change with temperature for the (1-x)KNBNNO-x$LiNbO_3$ (x = 0.00–0.08) ceramics at 10 kHz.

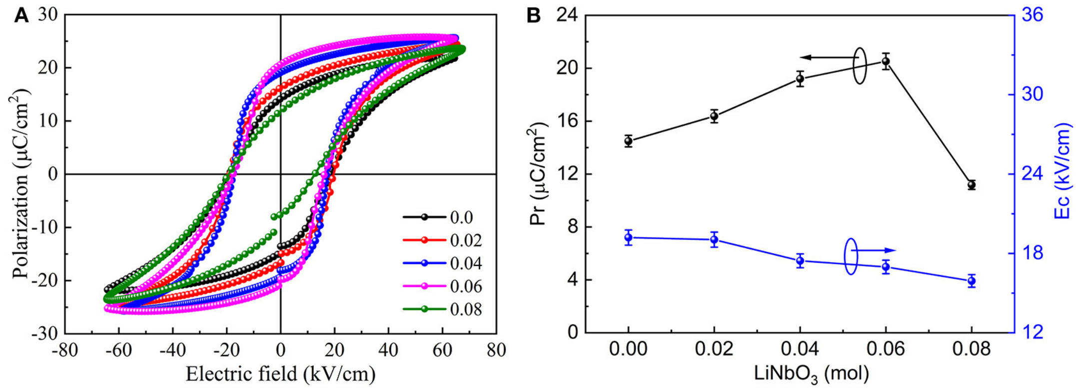

FIGURE 5 | (A) Polarization-electric field hysteresis loops of (1-*x*)KNBNNO-*x*$LiNbO_3$ (x = 0.00–0.08) ceramics at 10 Hz under room temperature; **(B)** *Pr* and *Ec* change with $LiNbO_3$ content.

10 kHz. The doping of $LiNbO_3$ could reduce the fluctuation, namely, enhancing the thermal stability of the (1-*x*)KNBNNO-*x*$LiNbO_3$ solid solution ($\Delta\varepsilon/\varepsilon_{40^\circ C} \leq \pm10\%$). As a result, the 0.94KNBNNO-0.06$LiNbO_3$ composition exhibits large relative permittivity (~1,400), optimum thermal stability ($\Delta\varepsilon/\varepsilon_{40^\circ C} \leq \pm10\%$) at 40–348°C, and low dielectric loss (<2.5%). It is well established that this composition will be a promising candidate for advanced smart devices operating at a broad temperature range.

The piezoelectric properties for the (1-*x*)KNBNNO-*x*$LiNbO_3$ (x = 0.00–0.08) ceramics are shown in **Figure 4**. The piezoelectric coefficient of the samples increase to an optimal value (~160 pC·N^{-1}) at x = 0.06, and then it drops to 147 pC·N^{-1} at x = 0.08. The pure KNBNNO composition also exhibits similar piezoelectric property compared with the existing results (Wang et al., 2013). The piezoelectric properties of the samples could be influenced by the existing of MPB (between orthorhombic and tetragonal). The emerging of more polarization vectors than that of single-phase favors more dipole reorientations, which largely improves the piezoelectric property (Wu et al., 2016; Xu et al., 2016; Acosta et al., 2017; Lv et al., 2019). Moreover, the piezoelectric property might be affected, to some extent, by the dense structure and grain size (Song et al., 2007).

Figure 5A illustrates the polarization-electric field hysteresis loops of the (1-*x*)KNBNNO-*x*$LiNbO_3$ (x = 0.00–0.08) ceramics at 10 Hz under room temperature. These samples exhibit typical P-E hysteresis loops. **Figure 5B** shows that the P_r value first slightly increases during x = 0.00–0.06 and then decreases to 11.18 μC·cm^{-1} at x = 0.08. The obtained maximum value of 20.5 μC·cm^{-2} appeared at x = 0.06. The E_c value decreases from 20 kV·cm^{-1} (x = 0.00) to 15 kV·cm^{-1} (x = 0.08). That can be ascribed to more polarization states caused by the coexistence of O-T phase at MPB, where domain wall movement would be easier and coercive field would be lower (Du et al., 2007a; Wang and Li, 2010b). On the other hand, when the grain size of samples increases with the improving of $LiNbO_3$ content, the density of grain boundary would decrease. Accordingly, the switching of the domain will much easier, leading to the reduction of the coercive field and increasing of remnant polarization. The piezoelectric and dielectric properties have a similar physical mechanism.

CONCLUSIONS

(1-*x*)KNBNNO-*x*$LiNbO_3$ ceramics (x = 0–0.08) were successfully synthesized via the traditional solid-state reaction method. The pure perovskite structure was obtained at $0 \leq x \leq 0.06$. However, the second phase of $K_3Li_2Nb_5O_{15}$ with tetragonal tungsten bronze structure was formed due to the solubility limit of Li-ions in the A-sites of solid solution (x = 0.08). There exist excellent piezoelectric and dielectric temperature stability properties with a high Curie temperature at $0.02 \leq x \leq 0.06$, owing to the formation of MPB between the orthorhombic and tetragonal phases. 0.94KNBNNO-0.06$LiNbO_3$ ceramics exhibits excellent electrical performance of ε_r~1400 ($\Delta\varepsilon/\varepsilon_{40^\circ C} \leq \pm10\%$), tan$\delta$ < 0.02 at 40–348°C, and d_{33} of ~160 pC N^{-1}, P_r of 20.5 μC cm^{-2} at room temperature. It is uncovered that this material could be used in energy, sensor, and smart devices, operating over a wide temperature range.

DATA AVAILABILITY STATEMENT

The datasets generated for this study are available on request to the corresponding author.

AUTHOR CONTRIBUTIONS

HJ and WL conceived and designed the experiments. HJ, HM, and ZC performed the experiments. LX, ZD, LP, and JX analyzed the data. HJ and LX wrote and revised the paper.

FUNDING

This work was supported by the National Natural Science Foundation of China (Grant No. 61601359), Key Science and Technology Program Funded by Shaanxi Province Science and Technology Bureau (Project No. 16JS038), Natural Science Basic Research Plan in Shaanxi Province of China (Project No. 2019JM-300), and Principal's Foundation from Xi'an Technological University (Project No. XAGDXJJ15003).

REFERENCES

Acosta, M., Novak, N., Rojas, V., Patel, S., Vaish, R., Koruza, J., et al. (2017). $BaTiO_3$-based piezoelectrics: Fundamentals, current status, and perspectives. *Appl. Phys. Rev.* 4:041305. doi: 10.1063/1.4990046

Bai, Y., Jantunen, H., and Juuti, J. (2018). Energy harvesting research: the road from single source to multisource. *Adv. Mater.* 30:1707271. doi: 10.1002/adma.201707271

Bai, Y., Tofel, P., Palosaari, J., Jantunen, H., and Juuti, J. (2017). A game changer: a multifunctional perovskite exhibiting giant ferroelectricity and narrow bandgap with potential application in a truly monolithic multienergy harvester or sensor. *Adv. Mater.* 29:1700767. doi: 10.1002/adma.201700767

Bai, Y., Xiang, H., Jantunen, H., and Juuti, J. (2019). Multi-functional perovskites–an investigation of compositional and processing influence on microstructure, dielectric and ferroelectric properties. *Eur. Phys. J-Spec. Top*. 228, 1555–1573. doi: 10.1140/epjst/e2019-800132-8

Bokov, A. A., and Ye, Z. G. (2012). Dielectric relaxation in relaxor ferroelectrics. *J. Adv. Dielectr.* 2:1241010. doi: 10.1142/S2010135X1241010X

Chang, Y., Yang, Z., Hou, Y., Liu, Z., and Wang, Z. (2007). Effects of Li content on the phase structure and electrical properties of lead-free $(K_{0.46-x/2}Na_{0.54-x/2}Lix)(Nb_{0.76}Ta_{0.20}Sb_{0.04})O_3$ ceramics. *Appl. Phys. Lett.* 90:232905. doi: 10.1063/1.2746411

Cheng, L. Q., Zhou, J. J., Wang, K., Li, J. F., and Wang, Q. M. (2012). Influence of ball milling on sintering behavior and electrical properties of (Li, Na, K)NbO_3 lead-free piezoceramics. *J. Mater. Sci.* 47, 6908–6914. doi: 10.1007/s10853-012-6635-4

Ding, Y., Zheng, T., Xie, R., Lv, X., Yin, J., and Wu, J. (2018). High-performance potassium sodium niobate-based lead-free materials without antimony. *J. Mater. Sci-Mater. El.* 29, 14487–14494. doi: 10.1007/s10854-018-9582-2

Du, H., Tang, F., Liu, D., Zhu, D., Zhou, W., and Qu, S. (2007a). The microstructure and ferroelectric properties of $(K_{0.5}Na_{0.5})NbO_3$-$LiNbO_3$ lead-free piezoelectric ceramics. *Mater. Sci. Eng. B*, 136, 165–169. doi: 10.1016/j.mseb.2006.09.031

Du, H., Zhou, W., Luo, F., Zhu, D., Qu, S., and Pei, Z. (2007b). An approach to further improve piezoelectric properties of $(K_{0.5}Na_{0.5})NbO_3$-based lead-free ceramics. *Appl. Phys. Lett.* 91:202907. doi: 10.1063/1.2815750

Evans, D. M., Schilling, A., Kumar, A., Sanchez, D., Ortega, N., Arredondo, M., et al. (2013). Magnetic switching of ferroelectric domains at room temperature in multiferroic PZTFT. *Nat. Commun.* 4:1534. doi: 10.1038/ncomms2548

Glazer, A. M. (1975). Simple ways of determining perovskite structures. *Acta Crystallograph. Sect. A Cryst. Phys. Diffr. Theoret. Gen. Crystallogr.* 31, 756–762. doi: 10.1107/S0567739475001635

Hao, J., Li, W., Zhai, J., and Chen, H. (2019). Progress in high-strain perovskite piezoelectric ceramics. *Mater. Sci. Eng. R*, 135, 1–57. doi: 10.1016/j.mser.2018.08.001

Hao, J., Xu, Z., Chu, R., Li, W., and Fu, P. (2015). Good temperature stability and fatigue-free behavior in Sm_2O_3-modified 0.948 $(K_{0.5}Na_{0.5})NbO_3$-0.052 $LiSbO_3$ lead-free piezoelectric ceramics. *Mater. Res. Bull.* 65, 94–102. doi: 10.1016/j.materresbull.2015.01.044

Hong, C. H., Kim, H. P., Choi, B. Y., Han, H. S., Son, J. S., Ahn, C. W., et al. (2016). Lead-free piezoceramics–Where to move on? *J. Mat.* 2, 1–24. doi: 10.1016/j.jmat.2015.12.002

Kim, J., Ryu, J., Jo, S. H., and Lee, H. (2016). Thermal stability and local atomic structure of $(Na_{0.5}K_{0.5})NbO_3$ doped $BaTiO_3$ ceramics. *Ceram. Int.* 42, 11739–11742. doi: 10.1016/j.ceramint.2016.04.093

Liu, H., Chen, J., Ren, Y., Zhang, L., Pan, Z., Fan, L., et al. (2015). Large photovoltage and controllable photovoltaic effect in $PbTiO_3$-$Bi(Ni_{2/3+x}Nb_{1/3-x})$ $O_{3-\delta}$ ferroelectrics. *Adv. Electron. Mater.* 1:1400051. doi: 10.1002/aelm.201400051

Liu, L., Huang, Y., Li, Y., Fang, L., Dammak, H., Fan, H., et al. (2012). Orthorhombic to tetragonal structural phase transition in $Na_{0.5}K_{0.5}NbO_3$-based ceramics. *Mater. Lett.* 68, 300–302. doi: 10.1016/j.matlet.2011.10.103

Liu, L., Knapp, M., Ehrenberg, H., Fang, L., Fan, H., Schmitt, L. A., et al. (2017). Average vs. local structure and composition-property phase diagram of $K_{0.5}Na_{0.5}NbO_3$-$Bi_{1/2}Na_{1/2}TiO_3$ system. *J. Eur. Ceram. Soc.* 37, 1387–1399. doi: 10.1016/j.jeurceramsoc.2016.11.024

Liu, L., Shi, D., Knapp, M., Ehrenberg, H., Fang, L., and Chen, J. (2014). Large strain response based on relaxor-antiferroelectric coherence in $Bi_{0.5}Na_{0.5}TiO_3$-$SrTiO_3$-$(K_{0.5}Na_{0.5})NbO_3$ solid solutions. *J. Appl. Phys.* 116:184104. doi: 10.1063/1.4901549

Long, C., Li, T., Fan, H., Wu, Y., Zhou, L., Li, Y., et al. (2016). Li-substituted $K_{0.5}Na_{0.5}NbO_3$-based piezoelectric ceramics: crystal structures and the effect of atmosphere on electrical properties. *J. Alloy. Compd.* 658, 839–847. doi: 10.1016/j.jallcom.2015.10.245

Lv, X., Wu, J., Zhao, C., Xiao, D., Zhu, J., Zhang, Z., et al. (2019). Enhancing temperature stability in potassium-sodium niobate ceramics through phase boundary and composition design. *J. Eur. Ceram. Soc.* 39, 305–315. doi: 10.1016/j.jeurceramsoc.2018.08.039

Mazhao, D., Xiao, D., Wu, J., and Zhu, J. (2015). Phase structure and electrical properties of $0.965(K_{0.45}Na_{0.55})_{0.95}Ag_{0.05}(Nb_{1-x}Sb_x)O_3$-$0.035Bi_{0.5}(Na_{0.5}Li_{0.5})_{0.5}ZrO_3$ lead-free ceramics. *J. Mater. Sci-Mater. El.* 26, 7309–7315. doi: 10.1007/s10854-015-3359-7

Saito, Y., and Takao, H. (2006). High performance lead-free piezoelectric ceramics in the (K,Na)NbO_3-$LiTaO_3$ solid solution system. *Ferroelectrics* 338, 17–32. doi: 10.1080/00150190600732512

Shi, D., Liu, L., Huang, Y., Fang, L., and Hu, C. (2014). Structure and electrical properties of LiF doped $0.996(0.95K_{0.5}Na_{0.5}NbO_3$-$0.05LiSbO_3)$-$0.004BiFeO_3$ piezoelectric ceramics. *Ferroelectrics* 467, 99–109. doi: 10.1080/00150193.2014.932543

Song, H. C., Cho, K. H., Park, H. Y., Ahn, C. W., Nahm, S., Uchino, K., et al. (2007). Microstructure and piezoelectric properties of (1–x) $(Na_{0.5}K_{0.5})NbO_3$-x$LiNbO_3$ ceramics. *J. Am. Ceram. Soc.* 90, 1812–1816. doi: 10.1111/j.1551-2916.2007.01698.x

Sun, X., Deng, J., Liu, L., Liu, S., Shi, D., Fang, L., et al. (2016). Dielectric properties of $BiAlO_3$-modified (Na, K, Li) NbO_3 lead-free ceramics. *Mater. Res. Bull.* 73, 437–445. doi: 10.1016/j.materresbull.2015.10.005

Wang, K., and Li, J. F. (2007). Analysis of crystallographic evolution in (Na,K)NbO_3-based lead-free piezoceramics by x-ray diffraction. *Appl. Phys. Lett.* 91:262902. doi: 10.1063/1.2825280

Wang, K., and Li, J. F. (2010a). Low-temperature sintering of Li-modified (K, Na) NbO_3 lead-free ceramics: sintering behavior, microstructure, and electrical properties. *J. Am. Ceram. Soc.* 93, 1101–1107. doi: 10.1111/j.1551-2916.2009.03532.x

Wang, K., and Li, J. F. (2010b). Domain engineering of lead-free Li-modified (K,Na)NbO_3 polycrystals with highly enhanced piezoelectricity. *Adv. Funct. Mater.* 20, 1924–1929. doi: 10.1002/adfm.201000284

Wang, K., Yao, F. Z., Jo, W., Gobeljic, D., Shvartsman, V. V., Lupascu, D. C., et al. (2013). Temperature-insensitive (K, Na)NbO_3-based lead-free piezoactuator ceramics. *Adv. Funct. Mater.* 23, 4079–4086. doi: 10.1002/adfm.201203754

Wu, B., Wu, H., Wu, J., Xiao, D., Zhu, J., and Pennycook, S. J. (2016). Giant piezoelectricity and high Curie temperature in nanostructured alkali niobate lead-free piezoceramics through phase coexistence. *J. Am. Ceram. Soc.* 138, 15459–15464. doi: 10.1021/jacs.6b09024

Xiao, H., Dong, W., Guo, Y., Wang, Y., Zhong, H., Li, Q., et al. (2019). Design for highly piezoelectric and visible/near-infrared photoresponsive perovskite oxides. *Adv. Mater.* 31:1805802. doi: 10.1002/adma.201805802

Xu, K., Li, J., Lv, X., Wu, J., Zhang, X., Xiao, D., et al. (2016). Superior piezoelectric properties in potassium–sodium niobate lead-free ceramics. *Adv. Mater.* 28, 8519–8523. doi: 10.1002/adma.201601859

Yan, H., Zhang, Z., Zhu, W., He, L., Yu, Y., Li, C., et al. (2004). The effect of (Li, Ce) and (K, Ce) doping in Aurivillius phase material $CaBi_4Ti_4O_{15}$. *Mater. Res. Bull.* 39, 1237–1246. doi: 10.1016/j.materresbull.2004.04.020

Yan, T., Han, F., Ren, S., Deng, J., Ma, X., Ren, L., et al. (2018c). Enhanced temperature-stable dielectric properties in oxygen annealed $0.85(K_{0.5}Na_{0.5})$ NbO_3-0.15 $SrZrO_3$ ceramic. *Mater. Res. Bull.* 99, 403–408. doi: 10.1016/j.materresbull.2017.11.040

Yan, T., Han, F., Ren, S., Ma, X., Fang, L., Liu, L., et al. (2018a). Dielectric properties of $(K_{0.5}Na_{0.5})NbO_3$-$(Bi_{0.5}Li_{0.5})ZrO_3$ lead-free ceramics as high-temperature ceramic capacitors. *Appl. Phys. A* 124:338. doi: 10.1007/s00339-018-1757-4

Yan, T., Ren, S., Ma, X., Han, F., Fang, L., Peng, B., et al. (2018b). Dielectric properties of $(Bi_{0.5}K_{0.5})ZrO_3$ modified $(K_{0.5}Na_{0.5})NbO_3$ ceramics as high-temperature ceramic capacitors. *J. Electron. Mater.* 47, 7106–7113. doi: 10.1007/s11664-018-6641-7

Yan, T., Sun, X., Deng, J., Liu, S., Han, F., Liu, X., et al. (2017). Dielectric and conductivity behavior of Mn-doped $K_{0.5}Na_{0.5}NbO_3$ single crystal. *Solid State Commun.* 264, 1–5. doi: 10.1016/j.ssc.2017.07.009

Zhang, S., Xia, R., Shrout, T. R., Zang, G., and Wang, J. (2006). Piezoelectric properties in perovskite $0.948(K_{0.5}Na_{0.5})NbO_3$-$0.052LiSbO_3$ lead-free ceramics. *J. Appl. Phys.* 100:104108. doi: 10.1063/1.2382348

Zhao, P., Zhang, B. P., and Li, J. F. (2007). Enhancing piezoelectric d_{33} coefficient in Li/Ta-codoped lead-free $(Na,K)NbO_3$ ceramics by compensating Na and K at a fixed ratio. *Appl. Phys. Lett.* 91:172901. doi: 10.1063/1.2794405

Zhao, Y., Liu, J., and Yan, D. (2019). Improved piezoelectric and strain performance of $Na_2B_4O_7$-doped (Li, K, Na) NbO_3 lead-free piezoceramics. *J. Mater. Sci.* 54, 1126–1135. doi: 10.1007/s10853-018-2906-z

Zheng, T., Wu, J., Xiao, D., and Zhu, J. (2018). Recent development in lead-free perovskite piezoelectric bulk materials. *Prog. Mater. Sci.* 98, 552–624. doi: 10.1016/j.pmatsci.2018.06.002

Zhong, H., Xiao, H., Jiao, N., and Guo, Y. (2019). Boosting piezoelectric response of KNN-based ceramics with strong visible-light absorption. *J. Am. Ceram. Soc.* 102, 6422–6426. doi: 10.1111/jace.16618

Zuo, R., Fang, X., and Ye, C. (2007). Phase structures and electrical properties of new lead-free $(Na_{0.5}K_{0.5})NbO_3$-$(Bi_{0.5}Na_{0.5})TiO_3$ ceramics. *Appl. Phys. Lett.* 90:092904. doi: 10.1063/1.2710768

Conflict of Interest: The authors declare that the research was conducted in the absence of any commercial or financial relationships that could be construed as a potential conflict of interest.